Science and Technology, 4 (1999) 71-78

Experimental Investigation and Failure Analysis of Fastened GRP under Bending Using Finite Element Method and Artificial Neural Networks

Abdennour C. Seibi* and Saleh M. Al-Alawi#

**Department of Mechanical Engineering and #Department of Electrical and Electronics Engineering, College of Engineering, Sultan Qaboos University, P.O.Box 33, Al-Khod 123, Muscat, Sultanate of Oman.*

التقصي المعملي وتحليل الإخفاق لمادة الألياف الصناعية المربوطة بتعريضها للإنحناء باستخدام طرق العناصر المحدودة والشبكات العصبية الإصطناعية

عبدالنور السايبي وصالح العلوي

خلاصة : تقدم هذه الورقة طريقة غير مسبوقة تتمثل بالتنبؤ في تحليل شكل القوة والإخفاق (الإنكسار) لمادة الألياف الزجاجية المقوية والمربوطة وذلك بتعريضها للإنحناء باستخدام طرق العناصر المحدودة (FEM) والشبكات العصبية الإصطناعية (ANN). فالخواص الميكانيكية للألياف الزجاجية المركبة والمقوية تم بحثها (تقصيها) بواسطة التجارب المعملية بتعريضها للإنحناء. لقد تم اخذ العينات التي تم اختبارها من شركة أميتيت عُمان، وهي شركة مصنعة تقع في منطقة الرسيل الصناعية بسلطنة عُمان. حيث اشتملت التجارب المعملية على تعريض العينة لإنحناء ثلاثي النقط كما تم تعريضها للإنحناء تحت حمل استاتي بربط الأطراف بطريقة ميكانيكية. فالنتائج المعملية اثبتت بأن مقاييس العينة (مثل مسافة امتداد الإنحناء، عرض العينة والخطوة) جميعها تؤثر على قوة وصلابة الألياف الزجاجية. فبواسطة استخدام العناصر المحدودة (FEM) والشبكات العصبية الإصطناعية (ANN) تم معرفة نوع وشكل الإخفاق (الإنكسار) وأماكن حدوثه على العينة وتم مقارنته بشكل جيد مع النتائج المعملية.

ABSTRACT: This paper presents a novel approach that predicts the strength and failure modes of jointed Glass Reinforced Polyester (GRP) samples under bending using Finite Element Method (FEM) and Artificial Neural Network (ANN). The mechanical behaviour of fastened glassfiber reinforced plastics composites under bending have been experimentally investigated. Samples were obtained from Amiantit Oman, a manufacturing company operating in Russail Industrial Zone in the Sultanate of Oman. The experimental program involved the conduct of three point bending tests as well as bending tests of mechanically fastened joints under static loads. The experimental results showed that the dimensions of the specimen such as the bending span length, specimen width, and specimen pitch affect GRP strength and stiffness. FEM and ANN results predicted accurately the types of failure modes and their locations along the specimens and compared well with the experimental results.

Composite materials have been receiving a widespread use in industry as an alternative to conventional materials. However, composite structures made of several connected parts by means of rivets, inserts, bolts, present serious problem to engineers when subjected to complex loading conditions where high stress concentrations near the joints may lead to unexpected failure. Therefore, in order to avoid such incidents from occurring, proper design procedures based on the stress analysis of such joints and the use of reliable predictive tools must be established.

Although GRP materials offer desirable characteristics, the presence of joints may raise serious concerns and important questions that must be answered. Though, considerable research work has been performed to examine the strength behaviour of GRP/GRE (Glass Reinforced Epoxy) bolted joints under uniaxial tension (Alfred, 1987; Hamada *et al*, 1987; Hao *et al*, 1978; Smith and Poscoe, 1988) by varying the joint geometry, none of the work has studied the effect of joint geometry on the flexural behaviour of GRP. In addition, the finite element method (Cooper and Turvey, 1995) has been used to study the stress analysis of joints under uniaxial loading only to identify the failure modes taking place in various joints geometry.

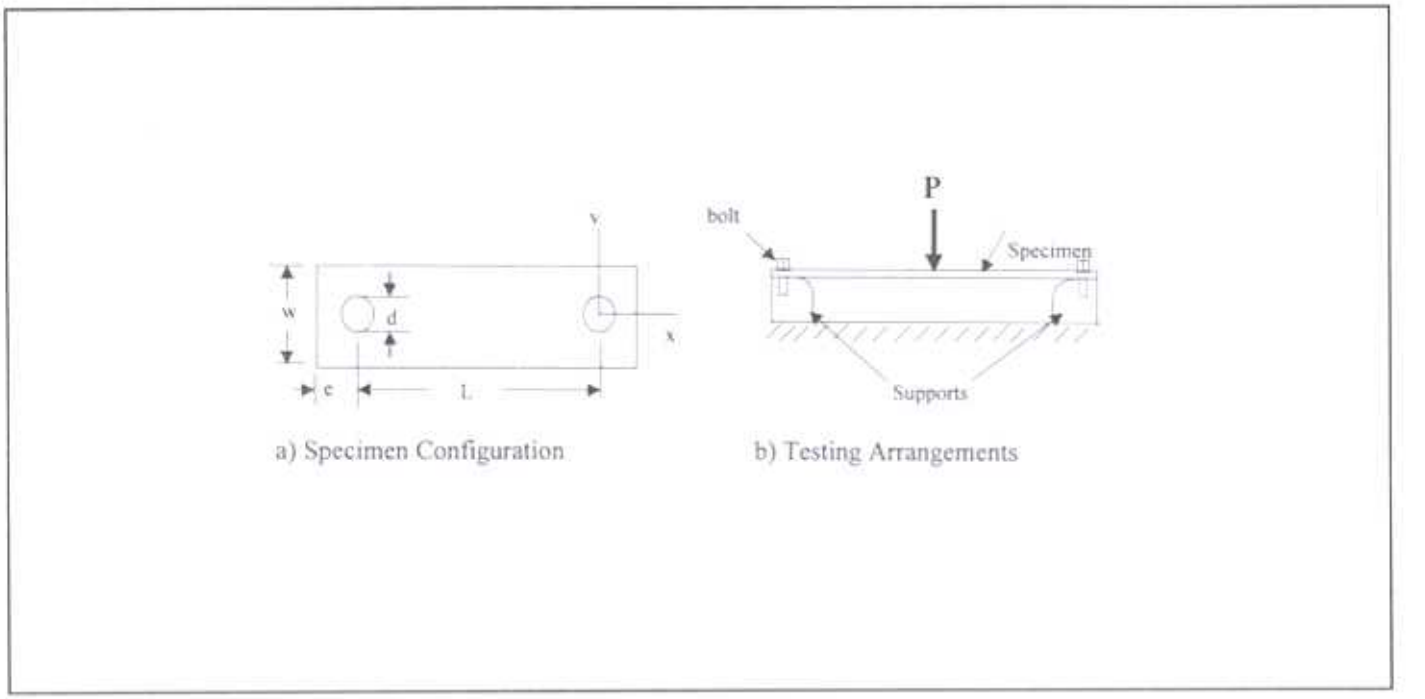

Figure 1. Bending Test of Fastened GRP Specimens.

The present paper, therefore, presents a novel approach that predicts the strength and failure modes of jointed Glass Reinforced Polyester samples under bending using the Finite Element Method (FEM) and the Artificial Neural Network (ANN) modeling technique. Identification of failure modes and their locations along the specimen in the neighbourhood of the joints was based on the maximum tensile stress obtained from the finite element analysis of fastened joints under bending.

Experimental Study

Laminates of 300x300x3 mm consisting of four layers of 50% weight fraction of random glass fibers mixed with polyester were fabricated in Amiantit Oman using the hand Lay-up Technique. The plates were then sandwiched between two wooden smooth plates to remove any trapped air and ensure a uniform distribution of polyester within the random fiber layers.

Standard three point bend specimens with various lengths, widths, and pitches were cut from cured plates. Holes of 8–mm diameter were drilled near the ends of the bend specimens as shown in Figure 1. Figure 1a shows the geometry of a typical specimen where L, e, and w are changed in the experiment. The span, L, the joint ratio w/d (specimen width/hole diameter), and e/d (center hole to edge distance/hole diameter) are changed from 70 to 160 mm, 1.5 to 2.25, and 0.75 to 1.5, respectively (see Table 2 for list of specimens). A schematic of the testing configuration is shown in Figure 1b where the specimen is fastened at both ends to a support by means of steel bolts. A static load was then applied at the center of the specimen span using a Lloyd M30K testing machine at a rate of 2-mm/ min. An X-Y plotter was used to plot the resulting load-deflection curves for different specimen configurations.

Experimental Results

An intensive experimental study was performed on more than 130 fastened specimens under bending to study the effects of joint geometry (Seibi, Al-Oraimi and Al-Alawi, 1996). It was reported that the general behaviour of the load-deflection curves becomes linear after a slight movement of the testing machine crosshead representing 1/10 (1 mm) of the total deflection of the tested specimen with no load being generated. In addition, four different failure modes were observed during testing. These failure modes consist of 1) bending mode (mode 1) corresponding to FPF (First Ply Failure) where failure takes place at the center of the specimen, 2) net tension (mode 2) where failure takes place at the sides of the joint, 3) bearing failure (mode 3) where damage initiates near the joint and continues to develop up to the failure of the joint and 4) mixed modes where failure takes place in the form of a combination of either modes 1&2 or modes 1&3 as shown in Figure 2.

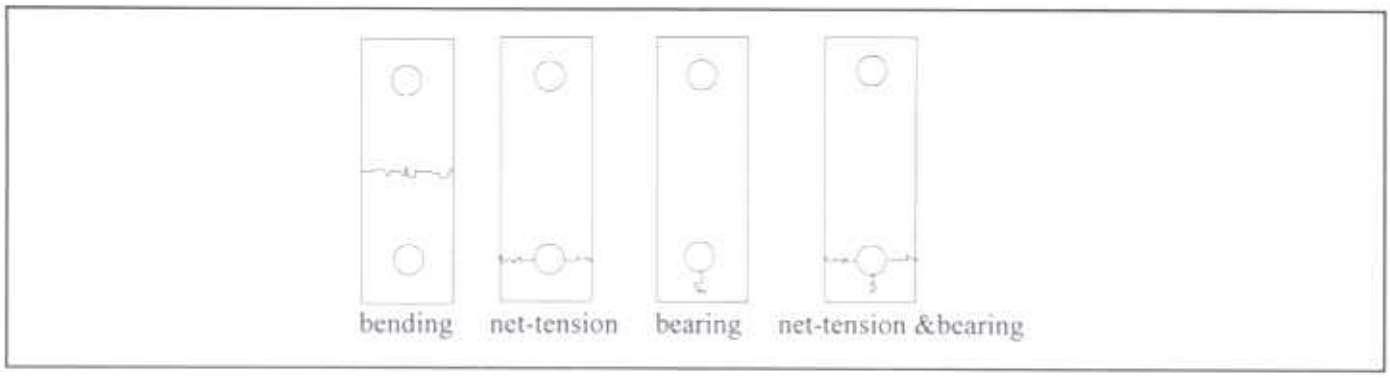

Figure 2. Failure Modes of Single Bolted Joints.

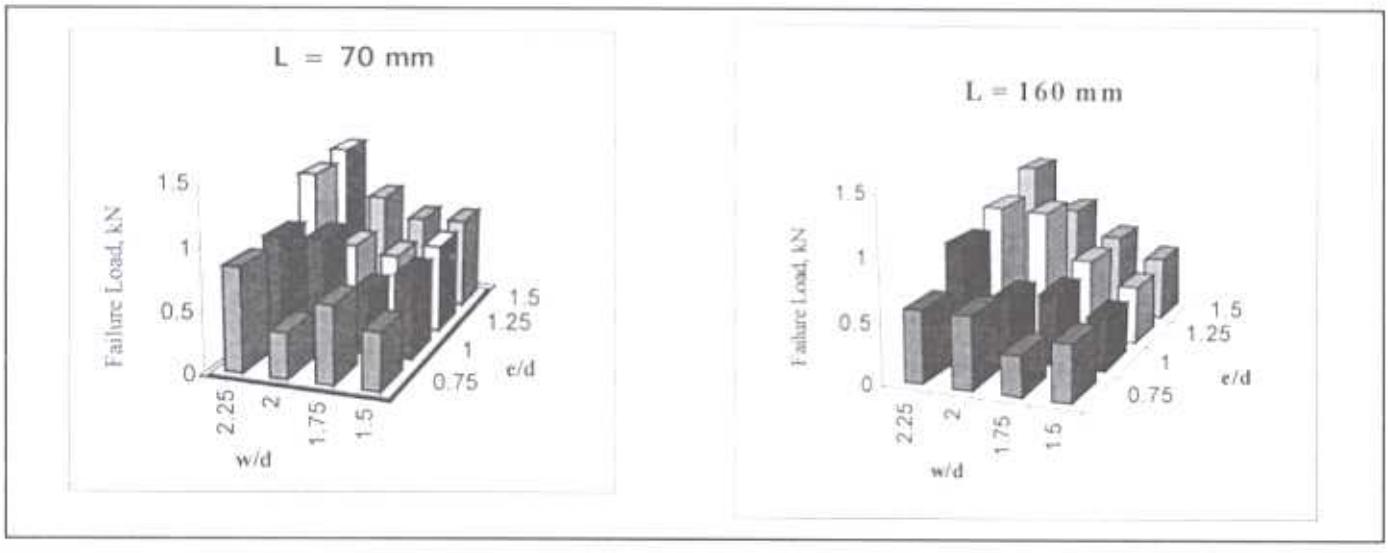

Figure 3. Effect of Joint Geometry on Failure Load of fastened GRP Under Bending.

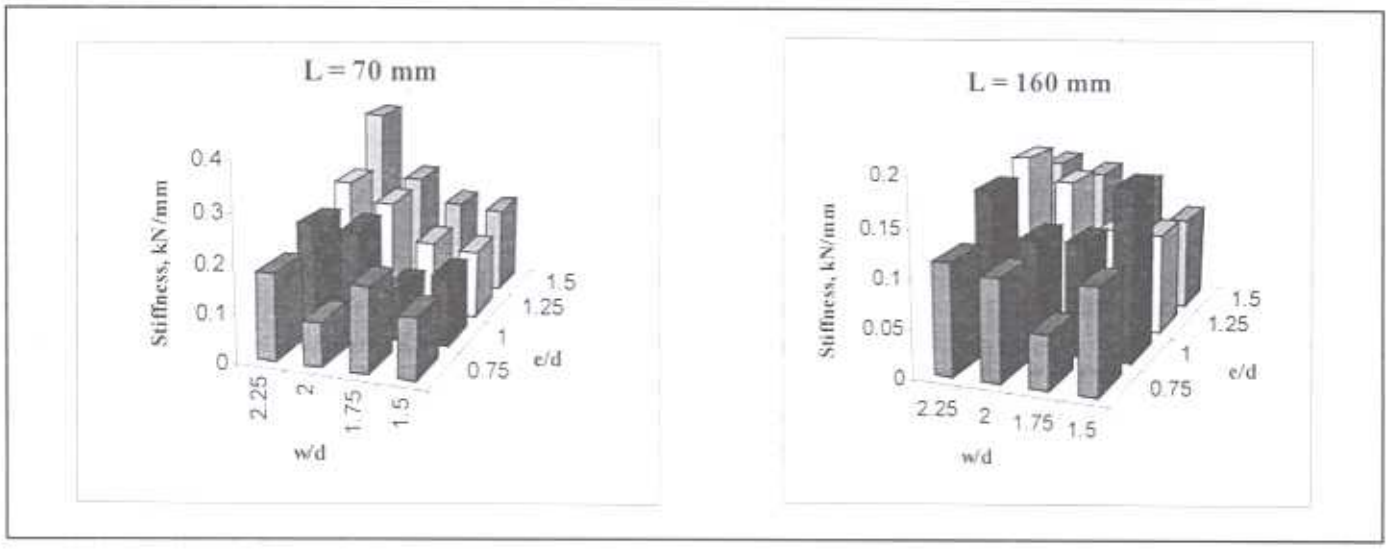

Figure 4. Effects of Joint Geometry on Initial Stiffness of Fastened GRP Under Bending.

The effects of joint geometry on the failure loads and bending stiffness with respect to the various bending spans can be seen in Figures 3 and 4. The bending stiffness is defined as the ratio of the applied to the corresponding deflection. These figures show the variation of the failure load and initial stiffness as functions of the width to hole diameter ratio, w/d, and pitch to diameter ratio, e/d, for the extreme bending spans of 70 and 160 mm. It can be seen that, in general, as w/d or e/d increases the failure load and initial stiffness increase implying that appropriate design parameters must be taken into consideration to avoid abrupt failure.

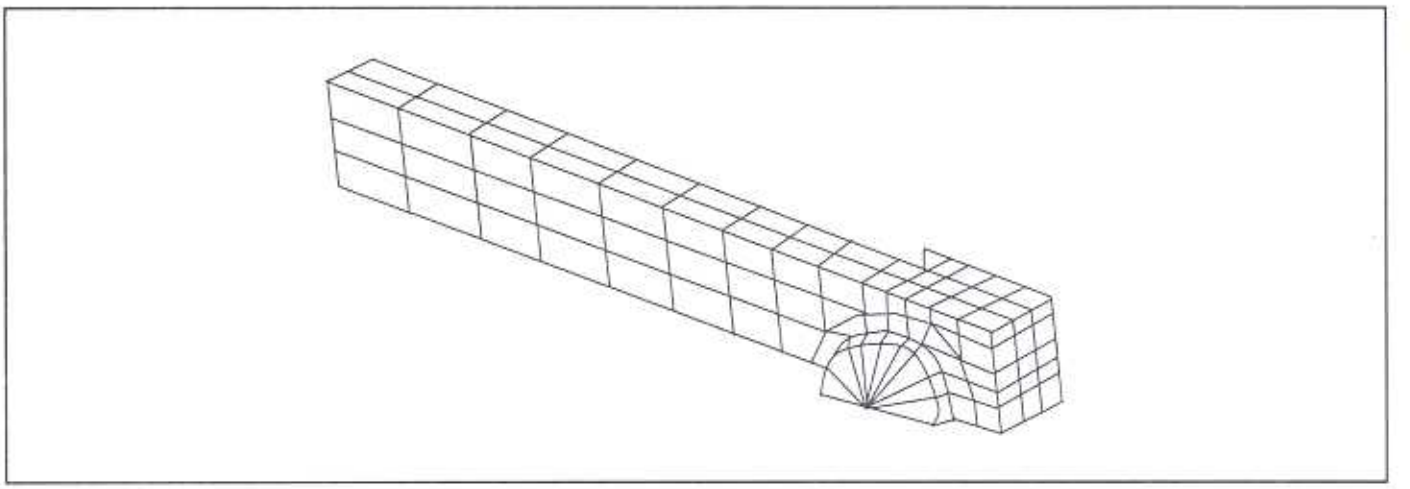

Figure 5. 3-D Finite element model of fastened GRP specimen.

Finite Element Analysis

The finite element analysis is used to identify the failure causes of the various failure modes observed experimentally by estimating the stress distribution near the joints of various specimen configurations under bending. The finite element analysis was conducted using a general-purpose finite element package ANSYS. The specimens which are made from randomly distributed glassfibers in plastic matrix materials, are assumed to behave transversely isotropic.

Finite Element Model

A three-dimensional brick was used to model the composite laminate, the support, and the bolt as shown in Figure 5 which presents a 3-D view of the model. Interaction between the sample and the bolt/support was taken into consideration by using a 3-D interface element. This element is capable of predicting the normal and tangential forces at the interface of all components by specifying the coefficient of friction and the normal and tangential stifnesses. The half circle in the model represents the bolt and the composite laminate with altered dimensions of w, e, and L consisting of two laminae with same material properties. Because of symmetry, only one fourth of the section of the laminate is considered. The Cartesian co-ordinates (x,y,z) represent x, y, and z-co-ordinates for the bend specimen configuration. The bolt has a radius of 4 mm and the composite laminate is 3 mm thick.

Boundary Conditions and Loading Procedure

The boundary conditions require a zero displacement for all the nodes lying on the x-z and y-z planes which represent the planes of symmetry. Only vertical motion along the z-axis is allowed for all nodes lying on the planes of symmetry. However, the rest of the nodes in the model are allowed to move freely in all directions. Since the finite element model, the applied load is taken as one fourth of the peak failure load taken from the load-deflection curves obtained experimentally. Concentrated forces are applied at the nodes lying on the surface at the specimens mid-span in the negative z-direction. The nodal forces are obtained by determining the applied force per unit width. Mesh refinement was performed before starting data generation of the resulting stresses near the joints. Examination of the stress distribution near the joints assists in predicting the location of impending failure.

Finite Element Results

The experimental results were supplemented by finite element modeling of a fastened GRP samples under bending. Stress analysis of joints was carried out using ANSYS finite element program. Stress distribution at the center of the bent specimen and near the joint along the radial direction in the x- and y-axes were examined to determine the expected type of failure and its location based on the maximum tensile stress theory.

It is believed that the driving stresses that cause failure at the joint sides and ends are the axial, σ_x , and lateral, σ_y, stresses, respectively. This hypothesis was based on the criterion that failure takes place at higher normal stresses to crack surface. In order to predict the location at which failure takes place, both axial and lateral stress distributions along the horizontal (x-axis) and vertical (y-axis) direction near the joint are plotted as shown in Figure 1. For instance, if the axial

stress (σ_x) along the vertical direction is higher than the lateral stress along the vertical direction (σ_y), failure is expected to occur along the y-axis (net tension mode), and if σ_y along the horizontal direction is greater than σ_x along the vertical direction, a bearing failure takes place. Figs. 6 and 7 show the maximum axial and lateral stresses for various ratios of e/d and w/d, respectively. In figure 6, it can be seen that the axial stress, σ_x denoted by Sx, is slightly affected by the ratio of e/d; however, the lateral stress, σ_y denoted by Sy, decreases as e/d increases. While it is noticeable that there is no change of the lateral stress with respect to the ratio of w/d, the axial stress decreases significantly for an increase in w/d (see Figure 7). Comparison between both stresses along both directions clearly specifies the location at which there is a high tendency of initial failure. For instance, Fig 6 shows that the axial stress is higher at a ratio of e/d = 0.75 implying that failure will take place at the end of the specimen representing a bearing failure. However, failure takes place at the side of the specimen (net tension failure) since the axial stress is higher than the lateral stress for higher ratios of e/d. On the other hand, Figure 7 shows that the axial stress at w/d ratios of 1.5, 1.75 is higher than the lateral stress implying that specimens with this geometric configuration fail from the sides (net tension mode). However, beyond these two ratios, specimens fail from the ends (bearing failure mode) since the lateral stress is higher than the axial stress. In addition, finite element results for other geometric configurations revealed that the maximum bending stress at mid span is higher than the first ply failure stress indicating that an FPF type of failure takes place at the center of the bent specimen. These results are not included in this paper because of the limited allowed space. A detailed finite element stress analysis of such joints is under investigation in order to understand the inter-relation between the failure modes and stress distribution around the joint. Future work will involve the development of a characteristic curve using finite element results from which failure modes and locations can be identified.

Ann Model Development

In this work, an ANN model was developed to predict the specimen failure strength, specimen stiffness, and failure location in fastened GRP specimens under bending. The model was based on experimental results obtained from testing variable specimen length, width, and pitch. Figure 8 shows the multilayer feedforward perceptron artificial neural network used in this study. The purpose of developing this model is to allow us to perform sensitivity analysis and to study the behaviour of the specimen geometry without having to resort to costly and time-consuming experiments, hence, providing both time and cost savings.

ANN Architectural Design

As illustrated by Figure 8, the network architecture is composed of many simple processing elements that are organized into a sequence of layers. These are the input layer, the hidden layer, and the output layer. The neurons in the input layer receive three input signals representing the specimen length (SL), specimen width (SW), and specimen pitch (SP); hence, three neurons were used for input in the ANN architecture. The output layer, on the other hand, consists of three output neurons representing the failure strength (FSG), stiffness (ST), and failure location in that specimen (FL). Between the input and output layers, generally, there is one or more hidden layers. Determining the number of hidden layers to use and the appropriate number of neurons to include in each hidden layer is not an exact science. Research in this area (Hecht-Nielsen, 1989; Lapedes and Farber, 1988) proved that one or two hidden layers with an adequate number of neurons is sufficient to model any solution surface of practical interest. As a result of evaluating a number of hidden node configurations and computing the root mean square error for both the design points

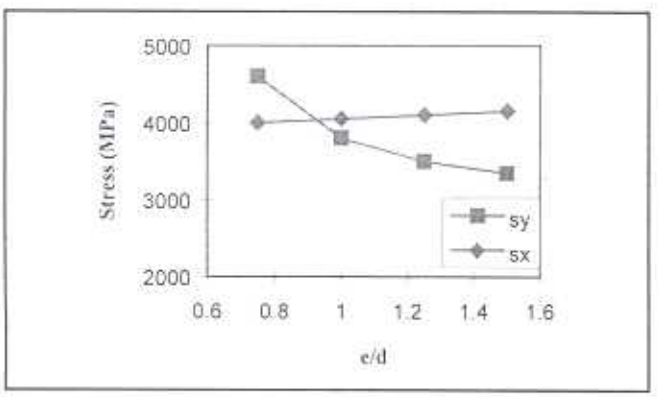

Figure 6. Effect of e/d on Type of Failure Modes.

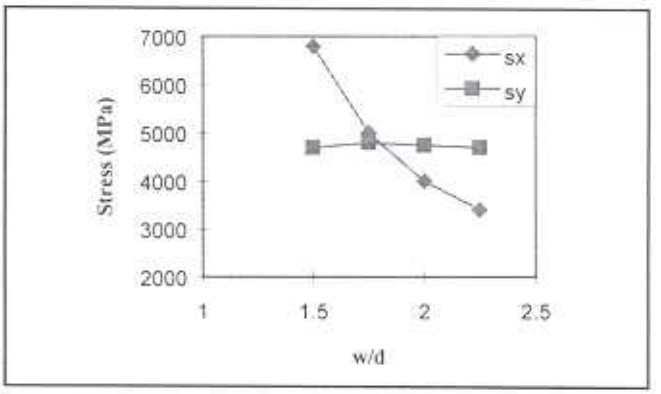

Figure 7. Effect of e/d on Type of Failure Modes.

and the test points, it was determined that a network with 7 to 10 nodes in the hidden layer would be a good choice. The network containing 9 hidden nodes, however, yielded the smallest error over the region of interest. Based on these results, one hidden layer containing 9 neurons was used to develop the ANN architecture.

Network Training

The multilayer feedforward network used in this work is trained using the backprobagation (BP) paradigm developed in reference (Rumelhart and McClelland, 1986). The BP algorithm uses the supervised training technique. In this technique, the interlayer connection weights and the processing element thresholds are first initialized to small random values. The network is then presented with a set of training patterns, each consisting of an example of the problem to be solved (the input) and the desired solution to this problem (the output). These training patterns are presented repeatedly to the ANN model, and weights are adjusted by small amounts that are dictated by the general delta rule (Rumelhart and McClelland, 1986). This adjustment is performed after each iteration when the networks computed output is different from the desired output. This process continues until weights converge to the desired error level or the output reaches an acceptable level. The system of equations that provides a generalized description of how the learning process is performed by the BP algorithm is described by Simpson (Simpson, 1990).

In the present work, the training process was performed using the NeuroShell® simulator. After several adjustments to the network parameters, the network converged to a threshold of 0.0001. The trained model prediction was in good agreement with the actual test results, hence, producing an R^2 value of 0.896 for the specimen failure strength (FSG), 0.838 for the stiffness (FST), and 0..991 for the failure location. These results show that approximately 91% of the variation in the dependent variables (output parameters) can be explained by the independent variables (input parameters) selected and the data set used. Having trained the network successfully the next step is to test the trained network, using the test data, in order to judge its performance.

TABLE 1

Examples of training patterns used in developing the ANN model

Parameter	Input	Input	Input	Output	Output	Output
Case Number	SL (mm)	SW (mm)	SP (mm)	FSG (KN)	FST (KN/mm)	Failure Location*
45	130	14	8	0.500	0.090	1
18	70	18	10	0.933	0.267	3
50	130	16	6	0.510	0.133	2
68	160	16	12	0.920	0.144	4

** Where Failure Location is 1 =bending, 2=net-tension 3=bearing, and 4=net-tension & bearing*

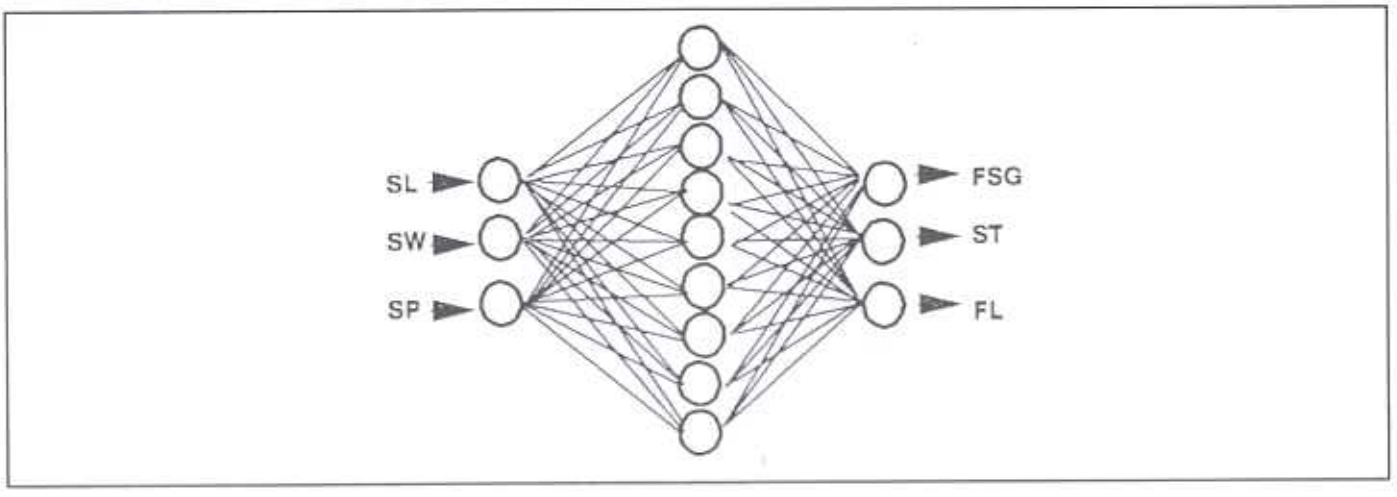

Figure 8. The Proposed ANN Model's Architecture.

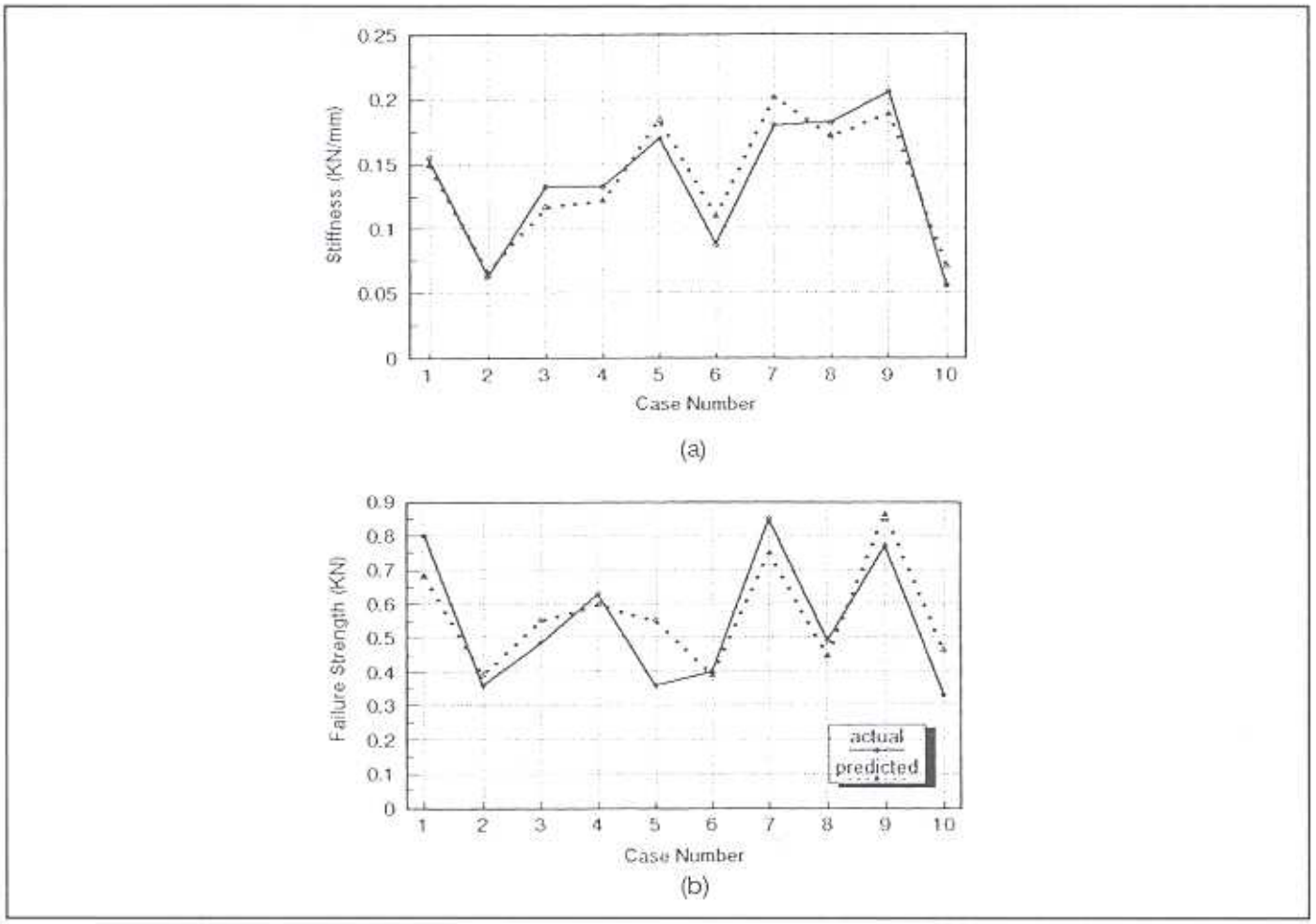

Figure 9. ANN prediction vs. actual experimental values for (a) stiffness and (b) strength.

Network Testing and Validation

The generalization capability of the model was also tested by presenting 10 test sets that were taken from the experimental data prior to network training. Figure 9 provide the results and illustrate the relationship between actual and predicted values for the specimen stiffness and failure strength. In addition, the model predicted failure location accurately, in 14 of the 16 cases. In the second case, the ANN prediction was not entirely incorrect since the ANN predicted the failure to be bending when, in reality the failure was net-tension & bending. Also in the fifth case the ANN prediction was net tension &, bending and the actual experimental results indicates that the case was bending.

Typical failure modes obtained experimentally and numerically for a particular span (L = 100 mm) with various joint geometry, is shown in Table 2. Other parameters such as first ply failure load, failure load, initial stiffness, and failure modes for the other spans are not included because of the limited space. It can be seen that the failure modes predicted by FEM and ANN are similar to the ones obtained experimentally.

To validate these results, four of the more common statistical indices, generally used to determine model accuracy and performance, were used. These parameters were mean absolute deviation (MAD), mean squared error (MSE), mean absolute percentage error (MAPE), and coefficient of determination (R^2). Statistical analysis of the results indicate that the R^2 value for the testing set was 0.752 for the specimen strength, 0..911 for the specimen stiffness, and 0.975 for the identification of the specimen failure location. The MAPE was 14.01, 10.71, and 3.26. These results demonstrate that the ANN-based model can predict the specimen strength, stiffness, and failure location with an accuracy of approximately 86, 89, and 97 percent, respectivel.

Once the ANN model is developed and it produces accurate results, contribution of the different independent variables to the variation of the dependent variable values can be obtained from the model using the NeuroShell(utility. Examination of the input variables' contribution revealed that the specimen width (SW) had a substantial influence (5 1%) on the variation in strength, stiffness, and the identification of the failure location. This result is followed by the effect of the specimen length (SL) of approximately 32%. On the other hand, the contribution of the specimen pitch was 17.0%.

TABLE 2

Comparative results of failure modes predicted by different techniques for L = 100 mm

Specimen No	w/d	E/d	Experimental	FEM	ANN
1	1.5	0.75	Bearing	Bearing	Bearing
2	1.5	1	Net tension & bending	Net tension & bending	Bearing
3	1.5	1.25	Net tension	Net tension	Net tension
4	1.5	1.5	Net tension	Net tension	Net tension
5	1.75	0.75	Bending	Bearing	Net tension & bending
6	1.75	1	Net tension	Net tension	Net tension
7	1.75	1.25	Bending & net tension	Bending & net tension	Bending & net tension
8	1.75	1.5	Net tension	Net tension	Net tension
9	2	0.75	Net tension	Net tension	Net tension
10	2	1	Bending	Bending	Bending
11	2	1.25	Bending & net tension	Bending & net tension	Bending & net tension
12	2	1.5	Bending & net tension	Bending & net tension	Bending & net tension
13	2.25	0.75	Bearing	Bearing	Bearing
14	2.25	1	Bending	Bearing	Bearing
15	2.25	1.25	Bending	Bearing	Bearing
16	2.25	1.5	Bending	Bearing	Bearing

Conclusions

An Experimental investigation and failure analysis of fastened GRP materials under bending using finite element method and Artificial Neural Networks were performed. It was observed that in general, the failure load and initial stiffness of the material increase as w/d and e/d ratios increase. The effect of changing the bending span is observed in terms of stiffness and failure load reduction as it increases from 70 to 160 mm. Four failure modes representing net tension, bearing, bending, and combined modes were observed. In addition it can be concluded that FEM and ANN prove to be reliable tools in studying the stress distribution and predicting potential failure modes and locations. The use of this advanced modeling tool, ANN, can result in extensive time and cost savings for the user.

References

ALFRED, R., 1987. On the Design of Prestressed and Non-Prestressed Bolted Joints is Glass Fiber Reinforced UP-Laminates. *Composite Structures*, **4**, Vol. 1, pp. 59-73.

COOPER, C., and TURVEY, G. J., 1995. Effects of Joint Geometry and Bolt Torque on the Structural performance of Single Bolt Tension joints in Pultruded GRP Sheet Material. *Composite Structures*, **32**, pp. 217-226.

HAMADA, H., MAEKAWA, Z., and HORINO, T., 1987. Study on Static and Long-Term Strength of Mechanically Fastened GFRP and CFRP. *Composite Structures*, **4**, Vol. 1,pp. 74-85.

HAO, S. V., DI MARIA, A., and FELDMAN D., 1978. Inserts for Fastening Sheet Molding Compounds. *Composite Structures*, **4**, pp. 86-99.

HECHT-NIELSEN, P., 1989. Theory of the Back probagation Neural Network, Proc., Int. Joint Conf. On Neural Networks, IEEE, Washington, D. C., Vol. 1, pp. 593-605.

LAPEDES, A., and FARBER, R., 1988. *How Neural Network Works, Neural Information Processing Systems*, American Institute of Physics, pp. 442-456.

RUMELHART DAVID E., and MCCLELLAND, JAMES L., 1986. *Parallel Distributed Processing: Exploration in the Microstructure of Cognition*, Vol. 1, Foundations, massachassetts, Massachassetts, MIT Press.

SEIBI, A. C., AL ORAIMI, S. K., AL ALAWI, S. M., 1996. Effects of Joint Geometry on the Flexural Behavior of Glass Rein forced Plastics, Proc. of the 1st Int. Conf. On Composite Science & Technology, Durban (South Affica), p p. 471-476.

SIMPSON PATRICK, K., 1990. *Artificial Neural Systems: Foundations, Paradigms, Applications, and Implementations*, First Edition, Elmsford, New York: Pergamon Press Inc.,

SMITH, P. A., PASCOE, K. J., 1988. Fatigue of Bolted Joints in (0/90) CFRP Laminates. *Composite Science and Technology*, **29**, pp. 45-69.

Received 15 August 1997
Accepted 10 June 1999